



**HAL**  
open science

# Superior Electrochemical Performance of Electropolymerized Self-Organized TiO<sub>2</sub> Nanotubes Fabricated by Anodization of Ti Grid

Vinsensia Ade Sugiawati, Florence Vacandio, Alina Galeyeva, A. Kurbatov,  
Thierry Djenizian

► **To cite this version:**

Vinsensia Ade Sugiawati, Florence Vacandio, Alina Galeyeva, A. Kurbatov, Thierry Djenizian. Superior Electrochemical Performance of Electropolymerized Self-Organized TiO<sub>2</sub> Nanotubes Fabricated by Anodization of Ti Grid. *Frontiers in Physics*, 2019, 7, 10.3389/fphy.2019.00179 . hal-02649494

**HAL Id: hal-02649494**

**<https://amu.hal.science/hal-02649494>**

Submitted on 29 May 2020

**HAL** is a multi-disciplinary open access archive for the deposit and dissemination of scientific research documents, whether they are published or not. The documents may come from teaching and research institutions in France or abroad, or from public or private research centers.

L'archive ouverte pluridisciplinaire **HAL**, est destinée au dépôt et à la diffusion de documents scientifiques de niveau recherche, publiés ou non, émanant des établissements d'enseignement et de recherche français ou étrangers, des laboratoires publics ou privés.



Distributed under a Creative Commons Attribution 4.0 International License

# Superior Electrochemical Performance of Electropolymerized Self-Organized TiO<sub>2</sub> Nanotubes Fabricated by Anodization of Ti Grid

Vinsensia A. Sugiawati<sup>1</sup>, Florence Vacandio<sup>2</sup>, Thierry Djenizian<sup>1\*</sup>, Alina Galejeva<sup>3</sup>, Andrey P. Kurbatov<sup>3\*</sup>

<sup>1</sup>École des Mines de Saint-Étienne - Campus Georges Charpak Provence, France, <sup>2</sup>Aix-Marseille Université, France, <sup>3</sup>Al-Farabi Kazakh National University, Kazakhstan

*Submitted to Journal:*  
Frontiers in Physics

*Specialty Section:*  
Physical Chemistry and Chemical Physics

*Article type:*  
Original Research Article

*Manuscript ID:*  
496158

*Received on:*  
05 Sep 2019

*Revised on:*  
19 Oct 2019

*Frontiers website link:*  
[www.frontiersin.org](http://www.frontiersin.org)

---

### *Conflict of interest statement*

The authors declare that the research was conducted in the absence of any commercial or financial relationships that could be construed as a potential conflict of interest

### *Author contribution statement*

VA S performed experiments, analyzed the experimental results and wrote the manuscript. VA S, AG, APK, FV and TD discussed experimental results. FV and TD supervised the works. All the authors contributed to the reading of paper and gave advice on the revision of the manuscript.

### *Keywords*

Anode, microbatteries, polymer electrolyte, Ti grid, TiO<sub>2</sub> nanotubes

### *Abstract*

Word count: 136

Self-organized TiO<sub>2</sub> nanotubes grown on Ti grid acting as anode for Li-ion microbatteries were prepared via an electrochemical anodization. By tuning the anodization time, the morphology and length of the nanotubes were investigated by scanning electron microscope. When the anodization time reached 1.5 h, the TiO<sub>2</sub>nts/Ti grid anode showed a well-defined nanotubes, which are stable, well adherent ~90 nm with a length of 1.88 μm. Due to their high surface utilization, surface area and material loading per unit area, TiO<sub>2</sub>nts /Ti grid anode using polymer electrolyte exhibited a high areal capacity of 376 μAh cm<sup>-2</sup> at C/10 rate and a stable discharge plateau at 1.8 V without using a polymer binder and conductive additive. The storage capacity of the TiO<sub>2</sub>nts/Ti grid after 10 cycles is fifteen times higher compared to previous reports using planar Ti foils.

### *Contribution to the field*

Dear Professor Galstyan In this work, we report the fabrication of self-organized TiO<sub>2</sub> nanotubes grown on Ti grid by anodization. By tuning the anodization time, well-defined nanotubes could be obtained, which are stable and well adherent. Due to their high surface utilization, surface area and material loading per unit area, TiO<sub>2</sub>nts /Ti grid anode using polymer electrolyte exhibited a high areal capacity of 376 μAh cm<sup>-2</sup> at C/10 rate and a stable discharge plateau at 1.8 V without using a polymer binder and conductive additive. More remarkably, the storage capacity of the TiO<sub>2</sub>nts/Ti grid after 10 cycles is fifteen times higher compared to previous reports using planar Ti foils. Considering the outstanding performance, we believe that the results could attract the interest of the scientists interested in the development of Li-ion batteries and we hope you can consider the manuscript for potential publication in Frontiers in Physics.

### *Ethics statements*

#### *Studies involving animal subjects*

Generated Statement: No animal studies are presented in this manuscript.

#### *Studies involving human subjects*

Generated Statement: No human studies are presented in this manuscript.

#### *Inclusion of identifiable human data*

Generated Statement: No potentially identifiable human images or data is presented in this study.

### *Data availability statement*

Generated Statement: The datasets generated for this study are available on request to the corresponding author.

1 **Enhanced** Electrochemical Performance of Electropolymerized Self-  
2 **Organized TiO<sub>2</sub> Nanotubes Fabricated by Anodization of Ti Grid**

3 Vinsensia Ade Sugiawati<sup>1</sup>, Florence Vacandio<sup>2</sup>, A. Galeyeva<sup>3</sup>, A. P. Kurbatov<sup>3</sup> and Thierry  
4 **Djenizian<sup>1\*</sup>**

5 <sup>1</sup> Mines Saint-Etienne, Center of Microelectronics in Provence, Department of Flexible Electronics,  
6 France

7 <sup>2</sup> Aix Marseille Université, CNRS, Electrochemistry of Materials Research Group, MADIREL, UMR  
8 7246, F-13397, Marseille Cedex 20, France

9• <sup>3</sup>Al-Farabi Kazakh National University, Center of Physical-Chemical Methods of Research and  
10 Analysis, Kazakhstan, Almaty, Tole bi str., 96A.

11 **\* Correspondence:**  
12 Corresponding Author  
13 thierry.djenizian@emse.fr

14 **Keywords: Anode, Microbatteries, Polymer electrolyte, Ti grid, TiO<sub>2</sub> nanotubes**

15  
16 **Abstract**

17 Self-organized TiO<sub>2</sub> nanotubes grown on Ti grid acting as anode for Li-ion microbatteries were  
18 prepared via an electrochemical anodization. By tuning the anodization time, the morphology and  
19 length of the nanotubes were investigated by scanning electron microscope. When the anodization time  
20 reached 1.5 h, the TiO<sub>2</sub>nts/Ti grid anode showed a well-defined nanotubes, which are stable, well  
21 adherent ~90 nm with a length of  $1.9 \pm 0.1 \mu\text{m}$ . Due to their high surface utilization, surface area and  
22 material loading per unit area, TiO<sub>2</sub>nts /Ti grid anode using polymer electrolyte exhibited a high areal  
23 capacity of  $376 \mu\text{Ah cm}^{-2}$  at C/10 rate and a stable discharge plateau at 1.8 V without using a polymer  
24 binder and conductive additive. The storage capacity of the TiO<sub>2</sub>nts/Ti grid after 10 cycles is fifteen  
25 times higher compared to previous reports using planar Ti foils.

26 **1. Introduction**

27 Due to their high energy density, no memory effect and long cycle life, rechargeable Li-ion batteries  
28 (LIBs) have been extensively used as power sources for many electronic devices [1–4]. More recently,  
29 all-solid-state microbatteries have attracted intense attention for powering miniaturized electronics  
30 such as wireless sensors and a wide range of applications for the Internet of Things (IoT) [5–8].  
31 Titanium dioxide (TiO<sub>2</sub>) is an attractive and versatile material that is used in many technologies due to  
32 its unique properties such as high surface area, electronic properties, biocompatibility, and  
33 environmental well-being [9,10]. Particularly, synthesis of nanostructured TiO<sub>2</sub> such as nanotubes,  
34 nanowires and nanofibers has raised interest lately compared to the conventional microstructures due  
35 to their high surface-to-volume ratio [11–13]. The first reports on the formation of self-organized  
36 nanotubes on titanium by Assefpour-Dezfuly et al. in 1984 [14] where Ti metal was firstly etched in  
37 alkaline peroxide, then anodized in chromic acid and later by Zwilling et al. in 1999 [15] reported on  
38 the formation of nanoporous anodized TiO<sub>2</sub> nanotubes in a fluoride containing electrolyte. Since then,  
39 TiO<sub>2</sub> nanotubes have been extensively explored in various fields, such as photocatalysis[16],  
40 sensors[17], dye sensitized solar cells[18] and energy storage device [19].

41 Various approaches, such as sol-gel, hydrothermal treatment, template assisted method,  
42 electrospinning and electrochemical anodization have been employed to prepare one-dimensional TiO<sub>2</sub>  
43 nanostructures [20]. However, self-organized TiO<sub>2</sub>nts formed by anodization method is preferred  
44 owing to their simplicity, better control over the nanotube morphology and low-cost [19,21]. Thus,  
45 pristine as well as chemically modified TiO<sub>2</sub>nts obtained by anodization have been used as negative  
46 electrodes for high performance Li-ion batteries [22–24]. Most studies on self-organized TiO<sub>2</sub>nts are  
47 focused on the planar surface, for instance Ti foil. The utilization of Ti grid as the substrate to  
48 synthesize the TiO<sub>2</sub>nts has been extensively studied owing to its flexibility and unique geometry  
49 [25,26]. Much attentions have been paid on the fabrication of the TiO<sub>2</sub>nts on Ti grid as photoanode,

50 possessing an enhanced performance in terms of photon absorption and electron collection efficiency  
51 compared to anodized Ti foil [27–29]. Previous studies have shown the use of TiO<sub>2</sub>nts /Ti grid in Dye  
52 Sensitized Solar Cells (DSSCs) can effectively improve the charge collection efficiency of  
53 approximately 3.15% [27]. Liu et al. fabricated vertically oriented TiO<sub>2</sub> nanotube arrays with  
54 controllable lengths on Ti grids by electrochemical anodization in ethylene glycol-based electrolyte  
55 and investigated their potential application as flexible electrodes for DSSCs [30]. The work reported  
56 by Motola et al. showed a high photocatalytic, antimicrobial and antibiofilm activities of the TiO<sub>2</sub>  
57 nanotube layers grown on Ti grid [31,32].

58 Despite a large number of reports published on the fabrication of self-organized TiO<sub>2</sub>nts and their  
59 applications, the use of TiO<sub>2</sub>nts /Ti grid as anode material has never been investigated with a polymer  
60 electrolyte to achieve the fabrication of all-solid-state microbatteries. To improve the performance of  
61 the TiO<sub>2</sub>nts anodes for Li-ion microbatteries, self-organized TiO<sub>2</sub>nts grown on Ti grid is considered as  
62 a great choice owing to its large aspect ratio of length to diameter, higher surface area and high Ti  
63 conversion into TiO<sub>2</sub>nts [33,34]. Hence, the self-organized TiO<sub>2</sub>nts anode provides more easily access  
64 for the Li ions, which improves the electrochemical performance of the microbatteries. Herein, we  
65 report the fabrication of a liquid-free microbattery using self-organized TiO<sub>2</sub>nts/Ti grid filled by an  
66 electropolymerized electrolyte. The effect of the anodic oxidation time on the formation of the TiO<sub>2</sub>nts  
67 were investigated by scanning electron microscopy and the electrochemical performances of the  
68 electropolymerized TiO<sub>2</sub>nts was also studied by cyclic voltammetry and galvanostatic  
69 charge/discharge cycling. Compared to planar Ti surfaces (i.e. foil and thin film), we confirm that the  
70 discharge capacity values obtained from TiO<sub>2</sub>nts supported on a Ti grid are strongly enhanced.

71

72

73 **2. Experimental**

74 **2.1. Synthesis of TiO<sub>2</sub> nanotubes**

75 The TiO<sub>2</sub>nts anodes were fabricated by the electrochemical anodization of a titanium grid (Good  
76 Fellow 0.57 mm thickness, 0.23 mm wire diameter). Before anodization, the Ti grids were cut to 1.3 x  
77 1.3 cm<sup>2</sup> in size and cleaned via sonication in acetone, isopropanol and methanol for 10 min each in  
78 order to remove any surface impurity. After drying the grids with compressed air, TiO<sub>2</sub>nts were grown  
79 by the anodization of Ti grid in an organic electrolyte containing 96.7 wt. % glycerol, 1.3 wt. % NH<sub>4</sub>F  
80 and 2 wt. % water [35]. All the anodization experiments were carried out at room temperature in a two-  
81 electrode system with a Ti grid as a working electrode and platinum (Pt) foil as a counter electrode.  
82 The working electrode was pressed against an O-ring of the electrochemical cell leaving approximately  
83 0.63 cm<sup>2</sup> exposed to the electrolyte. The distance between the working and counter electrodes was set  
84 to 2 cm and the anodization was performed at room temperature without stirring of the electrolyte  
85 during anodization. A constant voltage of 60 V was applied to the two-electrode electrochemical cell  
86 using a generator (ISO-TECH IPS-603) for 1, 1.5, 2.5 and 3 h, respectively. After anodization, the  
87 samples were dipped in 0.5 vol. % HF solution for 30 seconds in order to remove the residue of the  
88 electrolyte, washed with distilled water and dried using compressed air. The as-formed TiO<sub>2</sub>nts were  
89 annealed at 450 °C in air for 3 h with a heating rate of 5 °C min<sup>-1</sup> in order to obtain anatase phase.

90 **2.2. Electrochemical polymerization**

91 In order to achieve the electrodeposition of PMMA-PEG (poly methyl ether methacrylate-polyethylene  
92 glycol) polymer electrolyte, cyclic voltammetry was performed on the TiO<sub>2</sub>nts in a three-electrode  
93 system using a VersaSTAT 3 potentiostat (Princeton Applied Research), Ag/AgCl as the reference and  
94 Pt electrode as the counter electrode in an aqueous solution composed of 0.5 M of  
95 bis(trifluoromethanesulfone)imide (LiTFSI) and 0.5 M MMA-PEG (methyl ether methacrylate-

96 polyethylene glycol) with an average molecular weight of 500 g mol<sup>-1</sup>. Prior to electropolymerization,  
97 the aqueous solution containing the polymer electrolyte was purged with Argon gas for 10 min to  
98 remove dissolved oxygen. The cyclic voltammetry experiments were carried out for 100 cycles at the  
99 scan rate of 10 mV s<sup>-1</sup> in the potential window of -0.35 V to -1V vs. Ag/AgCl (saturated) [20,36].

### 100 **2.3. Characterizations**

101 The crystallinity of the synthesized samples was examined by X-ray diffraction (XRD). The XRD  
102 pattern was recorded at room temperature using a Siemens D5000 diffractometer equipped with copper  
103 anticathode (Cu K<sub>α</sub> radiation of 0.1506 nm wavelength was used with graphite monochromator). The  
104 diffractograms were analyzed by comparing with the JCPDS-ICDD database (Joint Committee on  
105 Powder Diffraction Standards International Centre for Diffraction Data). The morphology of TiO<sub>2</sub>nts  
106 was investigated by scanning electron microscopy (SEM) using a Carl Zeiss AG - ULTRA 55 SEM  
107 using an electron beam energy of 15 kV. The chronoamperometric test took place in a two-electrode  
108 electrochemical cell with Ti grid and Pt foil as a working and counter electrode, respectively, using  
109 PARSTAT 2273.

110 The Swagelok test cells were assembled in an Ar-filled glove box. In the half-cell system, TiO<sub>2</sub>nts  
111 electrodes were assembled against metallic Li foil using the gel electrolyte of the LiTFSI and MMA-  
112 PEG. The Li foil was cut in a circular shape with the diameter of 9 mm and 2 circular sheets (10 mm  
113 in diameter) of the gel electrolyte in the Whatman paper were used as separator. The cells were  
114 galvanostatically charged and discharged in the potential window of 1 – 3 V vs. Li/Li<sup>+</sup> at different  
115 current densities and cyclic voltammetry was performed at a scan rate of 0.1 mV s<sup>-1</sup> using a VMP3  
116 potentiostat-galvanostat (Bio Logic).

117

118



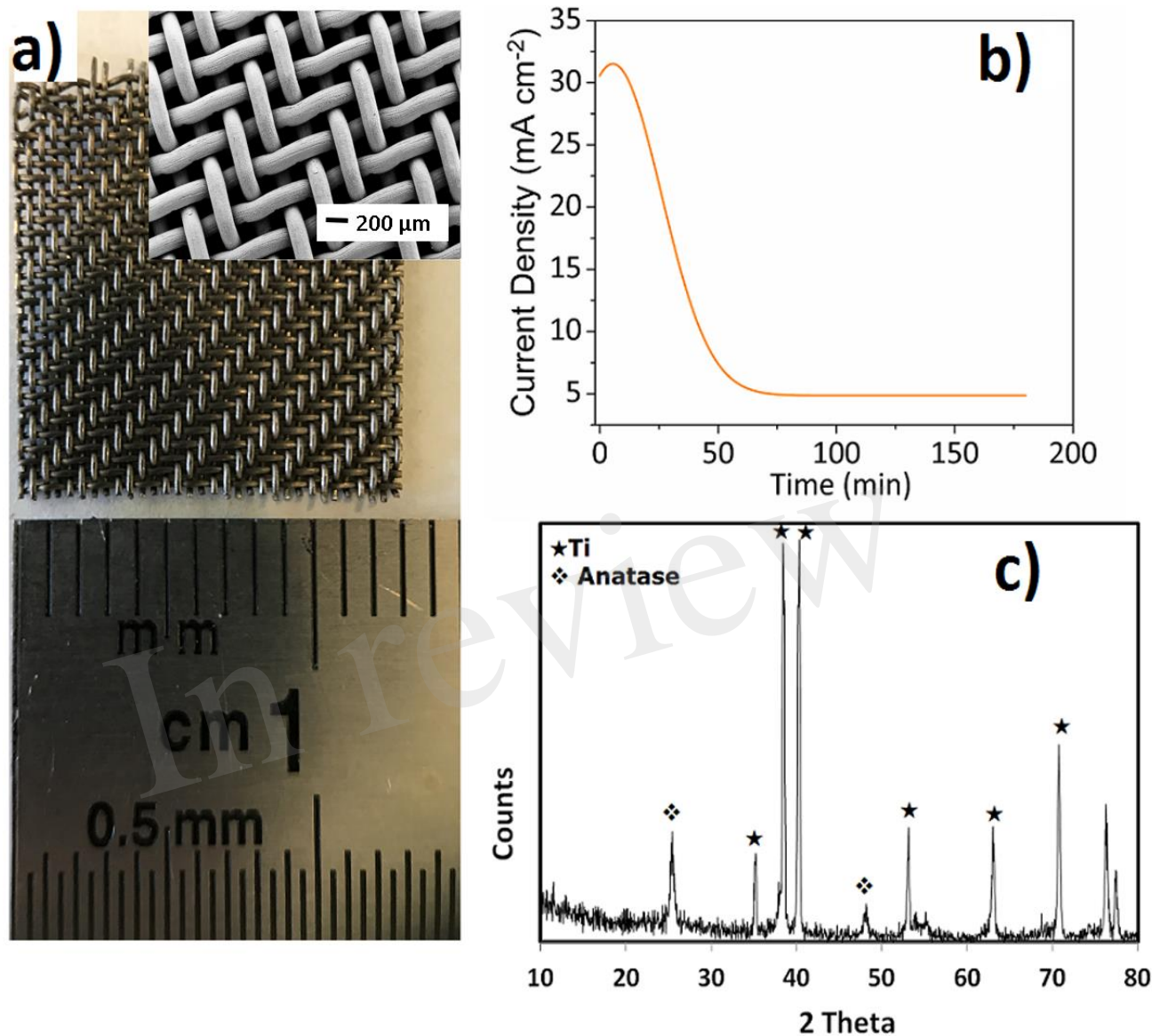
119 **3. Results and Discussion**

120 In this work, the growth of TiO<sub>2</sub> nanotubes was carried out by a low-cost and simple electrochemical  
121 anodization of Ti grid at different anodization time in a glycerol electrolyte containing fluoride ions  
122 and small amounts of water. **Figure 1a** shows the actual size of Ti grid used in the experiments and  
123 the inset shows the SEM image of the Ti grid. It can be seen Ti grid consist of many thin and radial Ti  
124 filaments which increase the surface area of the substrate. **Figure 1b** shows the chronoamperometric  
125 curve of Ti grid anodized at 60 V for 3 h. As seen, after a minor increase at the beginning of the  
126 anodization, the current density dropped with time due to the presence of an electrical barrier formed  
127 by the compact oxide layer. The minor increase in current density at the early stage of anodization  
128 might be attributed to the exposure of surface area that was not covered with the electrolyte due to the  
129 nature of the Ti grid structure. Self-organized TiO<sub>2</sub>nts starts to form as the result of the competition  
130 between electrochemical oxide formation and chemical dissolution of the oxide layer by fluoride ions  
131 according to **Equations 1 and 2**, respectively. Finally, steady current density was achieved when  
132 equilibrium was established between the growth and dissolution of the oxide layers [11].



135

136 The crystallinity of the TiO<sub>2</sub>nts was examined by XRD, as represented in **Figure 1c**. Immediately after  
137 growth the TiO<sub>2</sub>nts the tubes are amorphous and the formation of the anatase phase is obtained after  
138 annealing treatment. The presence of new peaks at about 25.3° and 47.9° correspond to the reflections  
139 of anatase phase (JCPDS file no. 21-1272). The Ti peaks observed on the XRD analysis are Ti substrate  
140 due to the direct growth of TiO<sub>2</sub>nts on the Ti grid. The residual Ti grid is directly used as the current  
141 collector.



142

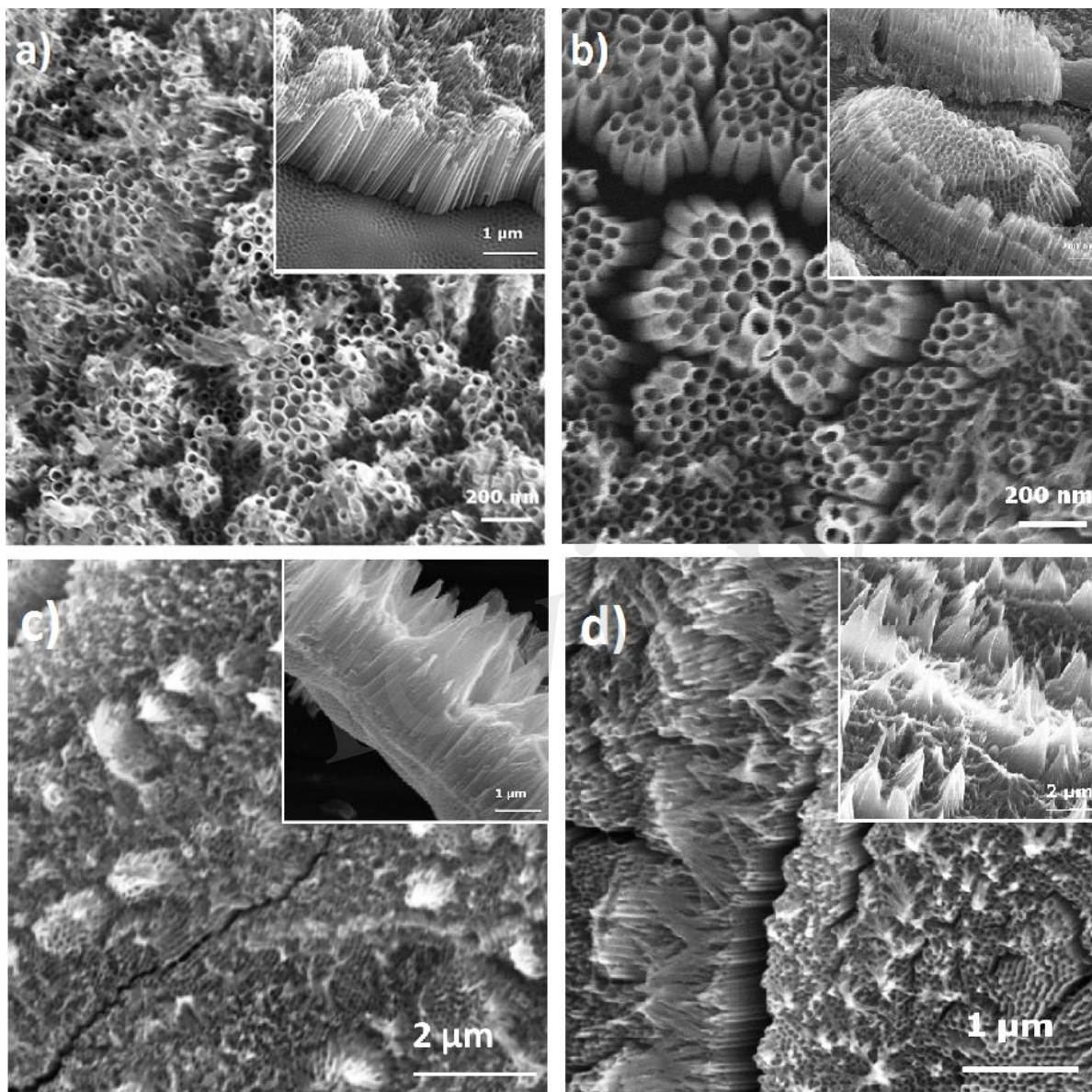
143 **Figure 1** a) Ti grid (inset: SEM image of Ti grid), b) chronoamperometric curve for the anodized Ti  
144 grid at applied potential of 60 V, and c) XRD patterns of TiO<sub>2</sub>nts annealed in air at 450 °C for 3 h.

145

146 In this work, effects of anodization time on the formation of TiO<sub>2</sub>nts arrays have been investigated.

147 **Figure 2a-d** illustrates how the morphology and length of the anodized layer evolve with the anodizing  
148 time. The SEM images show the top surface and cross-section morphologies of TiO<sub>2</sub>nts anodized at 60  
149 V for different durations of 1, 1.5, 2.5, and 3 h, respectively.

## Enhanced Electrochemical Performance of Electropolymerized Self-Organized TiO<sub>2</sub> Nanotubes Fabricated by Anodization of Ti Grid



150

151 **Figure 2** SEM images of TiO<sub>2</sub> nanotube arrays formed by electrochemical anodization of the Ti grid  
152 at 60 V for 1 h (a), 1.5 h (b), 2.5 h (c), and 3 h (d). Insets show the cross-sectional views.

153

154 As seen, some changes can be observed with **the increasing anodization time.** **For the shortest duration**  
155 (1 h), the nanotubes are clearly visible and the length of the nanotubes is ca.  $1.75 \pm 0.1 \mu\text{m}$  (**Figure**  
156 **2a**). However, the nanotube tops **are not enough homogenous and smooth** to ensure the conformal  
157 deposition of the polymer electrolyte. In **Figure 2b**, the SEM images showed the nanotubes anodized

## Enhanced Electrochemical Performances of Self-Organized TiO<sub>2</sub> Nanotubes Fabricated by Anodization of Ti Grid

158 for 1.5 h has an open-top structure without any bundle formation. The anodized Ti grid had  
159 comparatively longer and well-defined nanotubes, which are stable, well adherent to the grid substrate  
160 with a tube length of  $1.9 \pm 0.1 \mu\text{m}$ . Comparatively, 1.5 h and 1 h anodization does not show any bundle  
161 formation, yet, 1 h anodization showed shorter nanotubes than 1.5 h anodization. Indeed the collapse  
162 due to over dissolution of the top surface of nanotubes becomes very significant after 1.5 h. As a  
163 consequence, a substantial change in the morphology will affect the electrochemical performance of  
164 the electrodes. It is also observed that the length of the TiO<sub>2</sub>nts varies with the anodization time. The  
165 length of the TiO<sub>2</sub>nts increases as the anodization time **increases** from 1 h to 1.5 h, afterwards the length  
166 does not continue to increase with longer anodization time.

167 After longer anodization time (2.5 and 3 h), the nanotubes have closed-top structure and the bundled  
168 formation is found covering the entire top surface of the nanotubes. The thickness of the nanotubes  
169 layer after 2.5 h and 3 h anodization are  $1.8 \pm 0.2 \mu\text{m}$  and  $1.5 \pm 0.2 \mu\text{m}$ , respectively. Some studies  
170 showed that in long-duration anodization experiments, tubes can have inhomogeneous structures due  
171 to etching **of the top** [37]. The bundles on the tube tops might be formed due to the formation of needle-  
172 like morphologies as the walls may become too thin to support their own weight [11,38]. This bundle  
173 morphology is also described as nanograss or nanospike [39,40].

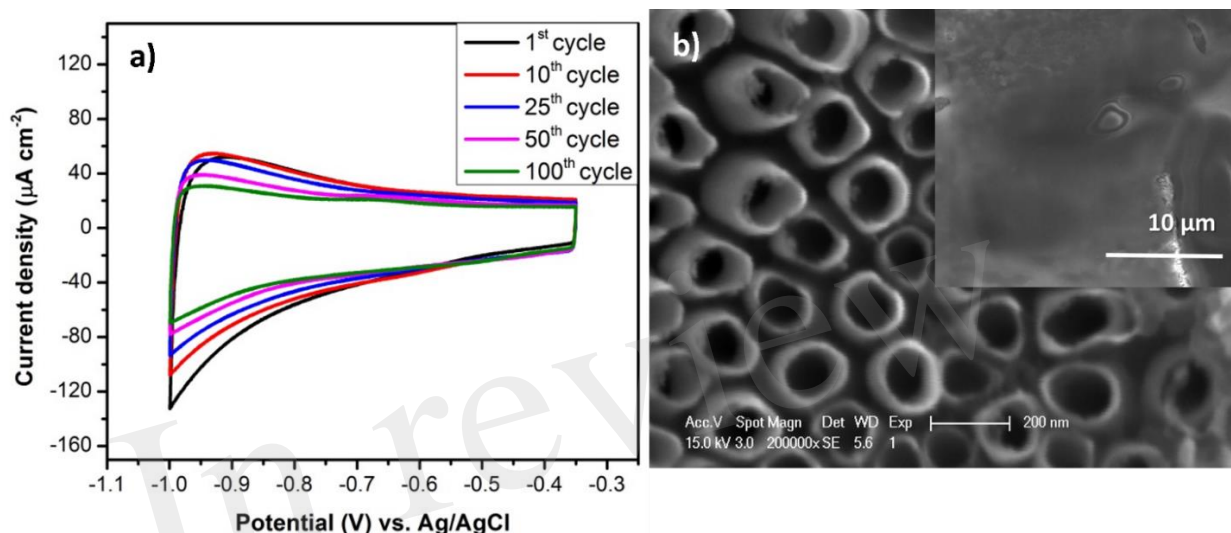
174 Nevertheless, **when the anodization time is decreased**, the **bundle formation** is disappeared. So, an  
175 appropriate oxidation time is the essential condition for the fabrication of highly ordered TiO<sub>2</sub> nanotube  
176 arrays onto Ti grid. These findings are in good agreement with the previous report. **Mor et al. reported**  
177 **that the nanotubes can grow longer by extending the anodization time, however the top of the nanotubes**  
178 **are gradually destroyed after extended anodization. The partial collapse of the nanotubes occurred due**  
179 **to an over dissolution reaction of the tubes top during the prolonged anodization, leading to the**  
180 **formation of bundled nanotubes [41,42]. Also, Zeng et al. reported that TiO<sub>2</sub> nanotubes grown on Ti**  
181 **grid showing a well-defined nanotubular structure after 20 minutes anodization, however the tubes top**

182 become fuzzy after prolonging the anodization time to 40 minutes [25]. Liu et al. [43] investigated the  
183 effect of the anodization time on the growth of TiO<sub>2</sub> nanotubes onto Ti grid at 60 V for 1-16 h and  
184 reported that the nanotube arrays grew uniformly after 3 h anodization. Additionally, as seen in Figure  
185 2, several fissures and bundling on the surfaces of the nanotubes could also be attributed to van der  
186 Waals attraction and capillary forces during drying [11,26,34].

187 Indeed, compared to Ti foils substrate, the intertwined structure of the Ti grid had more promising  
188 results in terms of surface area. As a result, the electrolyte can penetrate easily to the entire surface of  
189 the nanotubes that are radially grown in a 3-D array on the Ti grid [43,44]. Therefore, to further study  
190 the electrochemical performance of the self-organized TiO<sub>2</sub>nts/Ti grid, the TiO<sub>2</sub>nts/Ti grid anodized  
191 for 1.5 h was selected to be studied as anode for all-solid-state Li-ion microbatteries using PMMA-  
192 PEG polymer electrolyte.

193 After growing the TiO<sub>2</sub>nts on Ti grid substrate, the conformal electrodeposition of the electrolyte into  
194 nanotubes was achieved by the cyclic voltammetry (CV) technique. This approach is highly valuable  
195 to fully exploit the large surface area offered by the nanotubes through the formation of an augmented  
196 electrode/electrolyte interface [45–49]. **Figure 3** shows the cyclic voltammogram of the  
197 electropolymerization of the polymer electrolyte on the TiO<sub>2</sub>nts. The window of the applied cathodic  
198 potential was selected between the H<sub>2</sub> bubbling and the beginning of the proton reduction ( $-1 \text{ V} < E <$   
199  $E(\text{H}^+/\text{H}_2) = -0.551 \text{ V}$  vs. Ag/AgCl calculated from the Nernst equation) [46]. From cyclic  
200 voltammograms (CVs), as seen in **Figure 3a**, the absolute value of the cathodic current at -1 V vs.  
201 Ag/AgCl drops gradually with the increasing of cycles. The fading in the current can be explained by  
202 the successive deposition of the thin polymer layers that passivated the TiO<sub>2</sub>nts electrode. Additionally,  
203 the redox peaks of Ti<sup>4+</sup>/Ti<sup>3+</sup> are not observed and it is expected that there is no irreversible change in  
204 the oxidation states of Ti during the electropolymerization reaction. By using the same  
205 electrodeposition technique on the TiO<sub>2</sub>nts/Ti foil, Plylahan et. al.[47] reported that after 5 cycles CV,

206 the growth of a polymer layer occurred inside and outside of each nanotube walls. Indeed, after 10  
207 cycles CV, the inter-tube spaces are filled with the polymer and the nanotube walls become  
208 significantly thicker compared to the sample obtained after 5 cycle of CV. After 100 cycles, the  
209 polymer fills the inter-tube spaces and coats top surfaces of the TiO<sub>2</sub>nts/Ti grid (**Figure 3b**).



210

211 **Figure 3 a)** Cyclic voltammograms of TiO<sub>2</sub>nts electrode in 0.5M LiTFSI + 0.5M MMA-PEG500. The  
212 curves were recorded in the potential window of -0.35 to -1 V vs. Ag/AgCl (3M) at the scan rate of 10  
213  $\text{mV s}^{-1}$ , b) SEM images of the bare TiO<sub>2</sub>nts for 1.5 h and electropolymerized TiO<sub>2</sub>nts (inset).

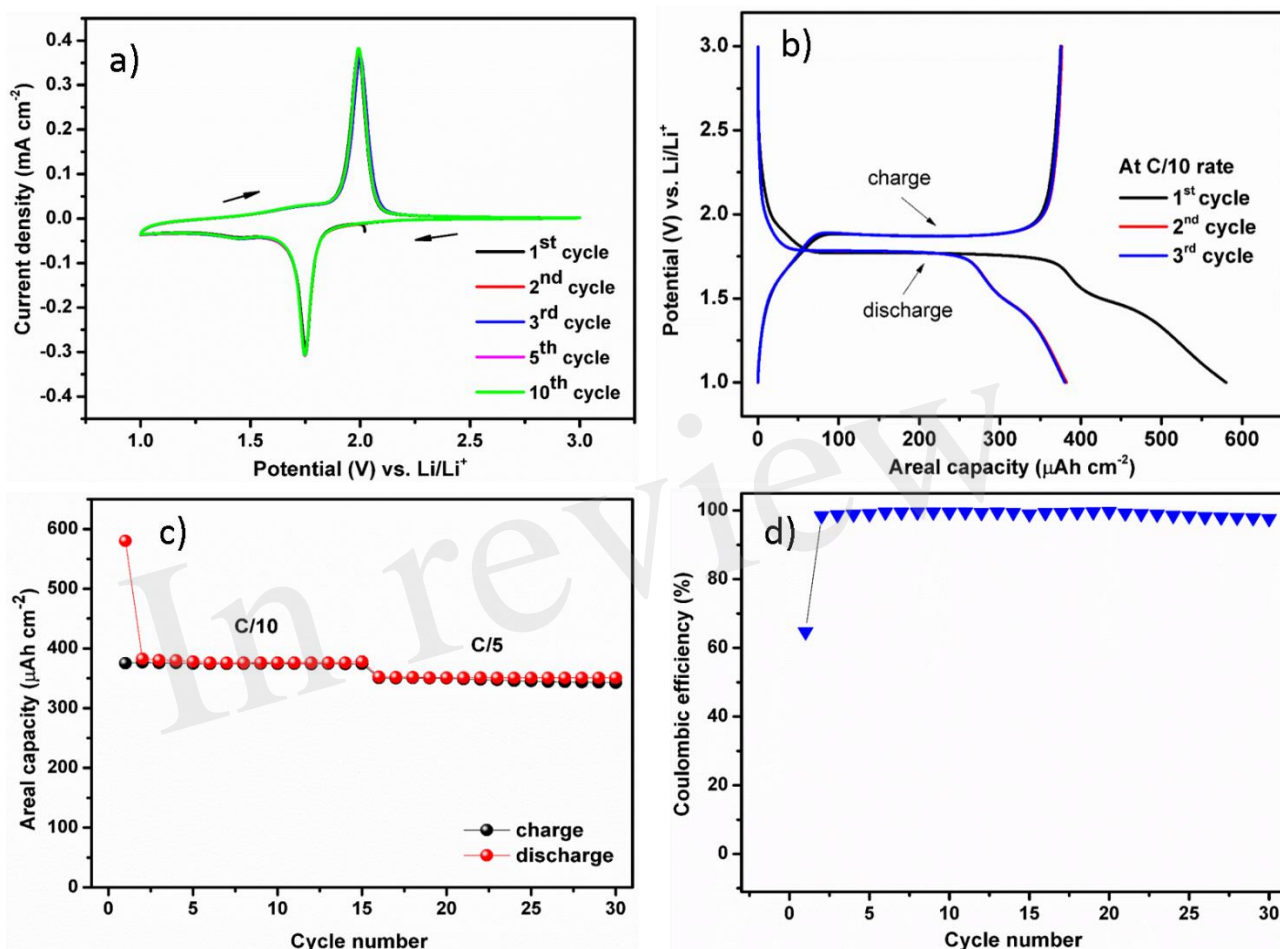
214

215 The CV experiments were performed to investigate the redox potential of TiO<sub>2</sub>nts electrodes. The CV  
216 curves were recorded at the scan rate of  $0.1 \text{ mV s}^{-1}$  between 1 and 3 V vs. Li/Li<sup>+</sup>. In **Figure 4a**, the two  
217 curves exhibit well-defined cathodic and anodic peaks at 1.75 and 1.98 V vs. Li/Li<sup>+</sup>, respectively,  
218 corresponding to lithium insertion/extraction potentials in anatase TiO<sub>2</sub>nts. The Li insertion/extraction  
219 process is reversible as seen in the unchanged shape of the CV curves upon cycling. The consecutive  
220 decrease in the absolute cathodic current indicates the slight discharge capacity fading upon cycling.

221 **Figure 4b** shows the galvanostatic charge/discharge profiles of the anatase TiO<sub>2</sub>nts. The profiles of

## Enhanced Electrochemical Performance of Electropolymerized Self-Organized TiO<sub>2</sub> Nanotubes Fabricated by Anodization of Ti Grid

222 each sample show flat plateaus of charge at 1.77 V vs. Li/Li<sup>+</sup> and discharge 1.88 V vs. Li/Li<sup>+</sup> which  
223 are typical profiles for the anatase TiO<sub>2</sub>nts.



224  
225 **Figure 4.** a) Cyclic voltammogram of anatase phase TiO<sub>2</sub>nts recorded at a scan rate of 0.1 mV s<sup>-1</sup> in  
226 the potential window of 1 V–3 V vs. Li/Li<sup>+</sup>, b) Galvanostatic charge/discharge profiles of the polymer-  
227 coated TiO<sub>2</sub>nts electrode, c) Capacity vs. cycle number of the polymer-coated TiO<sub>2</sub>nts electrode and  
228 d) Coulombic efficiency (%) the polymer-coated TiO<sub>2</sub>nts electrode.

229  
230 The cycling performance of anatase TiO<sub>2</sub>nts using the MMA-PEG500 gel electrolyte at C/10 and C/5  
231 rates are displayed in **Figure 4**. The areal capacities were calculated considering a density of anatase  
232 (4.23 g cm<sup>-3</sup>), a nanotube layer thickness (1.8 ± 2 μm) and an estimated porosity of 50% [36,50]. The

233 cell cycled between 1 and 3 V vs Li/Li<sup>+</sup> delivers an average capacity of ~376 μAh cm<sup>-2</sup> at C/10 and  
 234 ~350 μAh cm<sup>-2</sup> at C/5. The initial charge and discharge capacities of the electrodes are 375 μAh cm<sup>-2</sup>  
 235 and 580 μAh cm<sup>-2</sup>, corresponding to a relatively low initial coulombic efficiency of 64.7%. A large  
 236 irreversible capacity observed at the first cycles is attributed to the side reaction of Li<sup>+</sup> and the presence  
 237 of residual water at the surface of TiO<sub>2</sub>nts and in the polymer electrolyte. Additionally, some Li ions  
 238 are trapped inside the TiO<sub>2</sub> lattice structure after the first Li<sup>+</sup> insertion, thereby reducing the capacity  
 239 of the cell [35]. Nevertheless, for the subsequent cycles the capacities can be stabilized, the discharge  
 240 capacity values recorded in the 2nd and 3rd cycles are 382 and 380 μAh cm<sup>-2</sup> with improved coulombic  
 241 efficiency of 98.4 % and 98.7%, respectively. The cycling retention continuously enhanced after first  
 242 cycle and the coulombic efficiency approaches 100%.

243 The electrochemical performances of TiO<sub>2</sub>nts grown on Ti grid and Ti foil are summarized in **Table**  
 244 **1**. After 10 cycles, the storage capacity of the TiO<sub>2</sub>nts/Ti grid is fifteen times higher compared to our  
 245 previous report with Ti foils [14]. Calculated using a microbattery voltage of 1.8 V, the obtained areal  
 246 energy and power density of the TiO<sub>2</sub>nts/ Ti grid anode are 677 μWh cm<sup>-2</sup> and 67.7 μW cm<sup>-2</sup>,  
 247 respectively.

248 **Table 1.** Electrochemical performances of the microbatteries using PMMA-PEG polymer electrolyte

Electrodes	Areal Capacity at C/10 rate after 10 cycles (μAh cm <sup>-2</sup> )	V <sub>cell</sub> (V)	Energy density (μWh cm <sup>-2</sup> )	Power density (μW cm <sup>-2</sup> )
TiO <sub>2</sub> nts/ Ti foil [20]	25	1.7	43	4.3
TiO <sub>2</sub> nts/ Ti grid	376	1.8	677	67.7

249

250

251



252 **4. Conclusion**

253 To sum up, Ti grid is used as a 3D substrate to form self-organized TiO<sub>2</sub> nanotubes. The anodization  
254 time shows a significant influence on the morphological properties of the nanotubes. Well-defined  
255 nanotubes without bundle formation with a tube length of  $1.9 \pm 0.1 \mu\text{m}$  can be obtained after 1.5 h  
256 anodizing a Ti grid. Due to its radial and intertwined structure, Ti grid supplies much larger area than  
257 a Ti foil for a same footprint area. Actually, Ti grid showed much higher areal capacity in comparison  
258 to Ti foil at the same kinetics (C/10 and C/5). The main reason is because self-supported nanotubes are  
259 successfully formed within a very large surface area increasing the amount of the active material and  
260 the battery performance. After 10 cycles, the storage capacity of the TiO<sub>2</sub>nts/Ti grid is fifteen times  
261 higher compared to our previous report with Ti foils.

262  
263 **Author Contribution**

264 VA S performed experiments, analyzed the experimental results and wrote the manuscript. VA S, AG,  
265 APK, FV and TD discussed experimental results. FV and TD supervised the works. All the authors  
266 contributed to the reading of paper and gave advice on the revision of the manuscript.

267 **Conflict of Interest Statement**

268 The authors declare that the research was conducted in the absence of any commercial or financial  
269 relationships that could be construed as a potential conflict of interest.

270  
271 **Acknowledgment**

272 We acknowledge Région Sud for the financial support.

273  
274 **References**

- 275 1. Baggetto L, Knoops HCM, Niessen RAH, Kessels WMM, Notten PHL. 3D negative electrode  
276 stacks for integrated all-solid-state lithium-ion microbatteries. *J Mater Chem* (2010) **20**:3703–  
277 3708.

**Enhanced Electrochemical Performances of Self-Organized TiO<sub>2</sub> Nanotubes  
Fabricated by Anodization of Ti Grid**

- 278 2. Armand M, Tarascon J-M. Building better batteries. *Nature* (2008) **451**:652–657.
- 279 3. Sugiawati VA, Vacandio F, Eyraud M, Knauth P, Djenizian T. Porous NASICON-Type  
280 Li<sub>3</sub>Fe<sub>2</sub>(PO<sub>4</sub>)<sub>3</sub> Thin Film Deposited by RF Sputtering as Cathode Material for Li-Ion  
281 Microbatteries. *Nanoscale Res Lett* (2016) **11**.
- 282 4. Sugiawati VA, Vacandio F, Knauth P, Djenizian T. Sputter-Deposited Amorphous LiCuPO<sub>4</sub> Thin  
283 Film as Cathode Material for Li-ion Microbatteries. *ChemistrySelect* **3**:405–409.  
284 doi:10.1002/slct.201702429
- 285 5. Ferrari S, Loveridge M, Beattie SD, Jahn M, Dashwood RJ, Bhagat R. Latest advances in the  
286 manufacturing of 3D rechargeable lithium microbatteries. *J. Power Sources* (2015) **286**:25–46.
- 287 6. Nasreldin M, Delattre R, Ramuz M, Lahuec C, Djenizian T, de Bougrenet de la Tocnaye J-L.  
288 Flexible Micro-Battery for Powering Smart Contact Lens. *Sensors* (2019) **19**:2062.
- 289 7. Zheng S, Wu Z-S, Zhou F, Wang X, Ma J, Liu C, He Y-B, Bao X. All-solid-state planar integrated  
290 lithium ion micro-batteries with extraordinary flexibility and high-temperature performance.  
291 *Nano Energy* (2018) **51**:613–620.
- 292 8. Oudenhoven JFM, Baggetto L, Notten PHL. All-Solid-State Lithium-Ion Microbatteries: A  
293 Review of Various Three-Dimensional Concepts. *Adv. Energy Mater.* (2011) **1**:10–33.
- 294 9. Jaroenworarluck A, Regonini D, Bowen CR, Stevens R, Allsopp D. Macro, micro and  
295 nanostructure of TiO<sub>2</sub> anodised films prepared in a fluorine-containing electrolyte. *J.Mater. Sci.e*  
296 (2007) **42**:6729–6734.
- 297 10. Fraoucene H, Sugiawati VA, Hatem D, Belkaid MS, Vacandio F, Eyraud M, Pasquinelli M,  
298 Djenizian T. Optical and Electrochemical Properties of Self-Organized TiO<sub>2</sub> Nanotube Arrays  
299 From Anodized Ti–6Al–4V Alloy. *Front Chem.* (2019) **7**.
- 300 11. Roy P, Berger S, Schmuki P. TiO<sub>2</sub> nanotubes: Synthesis and applications. *Angew. Chem. Int. Ed.*  
301 (2011) **50**:2904–2939.
- 302 12. Krysa J, Lee K, Pausova S, Kment S, Hubicka Z, Ctvrtlik R, Schmuki P. Self-organized  
303 transparent 1D TiO<sub>2</sub> nanotubular photoelectrodes grown by anodization of sputtered and  
304 evaporated Ti layers: A comparative photoelectrochemical study. *Chem.Eng. J.* (2017) **308**:745–  
305 753.
- 306 13. Galstyan V, Vomiero A, Comini E, Faglia G, Sberveglieri G. TiO<sub>2</sub> nanotubular and nanoporous  
307 arrays by electrochemical anodization on different substrates. *RSC Adv.* (2011) **1**:1038–1044.
- 308 14. Assefpour-Dezfuly M, Vlachos C, Andrews EH. Oxide morphology and adhesive bonding on  
309 titanium surfaces. *J. Mater. Sci.* (1984) **19**:3626–3639.
- 310 15. Zwilling V, Darque-Ceretti E, Boutry-Forveille A, David D, Perrin MY, Aucouturier M. Structure  
311 and physicochemistry of anodic oxide films on titanium and TA6V alloy. *Surf. Interface Anal.*  
312 (1999) **27**:629–637.

## Enhanced Electrochemical Performance of Electropolymerized Self-Organized TiO<sub>2</sub> Nanotubes Fabricated by Anodization of Ti Grid

- 313 16. Zhou X, Liu N, Schmuki P. Photocatalysis with TiO<sub>2</sub> Nanotubes: “Colorful” Reactivity and  
314 Designing Site-Specific Photocatalytic Centers into TiO<sub>2</sub> Nanotubes. *ACS Catal.* (2017) **7**:3210–  
315 3235.
- 316 17. Galstyan V, Comini E, Baratto C, Ferroni M, Poli N, Faglia G, Bontempi E, Brisotto M,  
317 Sberveglieri G. Two-phase Titania Nanotubes for Gas Sensing. *Procedia Eng.* (2014) **87**:176–  
318 179.
- 319 18. Shankar K, Mor GK, Prakasam HE, Varghese OK, Grimes CA. Self-Assembled Hybrid  
320 Polymer–TiO<sub>2</sub> Nanotube Array Heterojunction Solar Cells. *Langmuir* (2007) **23**:12445–12449.
- 321 19. Ellis BL, Knauth P, Djenizian T. Three-Dimensional Self-Supported Metal Oxides for Advanced  
322 Energy Storage. *Adv. Mater.* (2014) **26**:3368–3397.
- 323 20. Plylahan N, Letiche M, Samy Barr MK, Ellis B, Maria S, Phan TNT, Bloch E, Knauth P,  
324 Djenizian T. High energy and power density TiO<sub>2</sub> nanotube electrodes for single and complete  
325 lithium-ion batteries. *J. Power Sources* (2015) **273**:1182–1188.
- 326 21. Macák JM, Tsuchiya H, Schmuki P. High-aspect-ratio TiO<sub>2</sub> nanotubes by anodization of  
327 titanium. *Angew. Chem. Int. Ed.* (2005) **44**:2100–2102. doi:10.1002/anie.200462459
- 328 22. Sopha H, Salian GD, Zazpe R, Prikryl J, Hromadko L, Djenizian T, Macak JM. ALD Al<sub>2</sub>O<sub>3</sub>-  
329 Coated TiO<sub>2</sub> Nanotube Layers as Anodes for Lithium-Ion Batteries. *ACS Omega* (2017) **2**:2749–  
330 2756.
- 331 23. Salian GD, Krbal M, Sopha H, Lebouin C, Coulet M-V, Michalicka J, Hromadko L, Tesfaye AT,  
332 Macak JM, Djenizian T. Self-supported sulphurized TiO<sub>2</sub> nanotube layers as positive electrodes  
333 for lithium microbatteries. *Appl. Mater. Today* (2019) **16**:257–264.
- 334 24. Salian GD, Koo BM, Lefevre C, Cottineau T, Lebouin C, Tesfaye AT, Knauth P, Keller V,  
335 Djenizian T. Niobium Alloying of Self-Organized TiO<sub>2</sub> Nanotubes as an Anode for Lithium-Ion  
336 Microbatteries. *Adv. Mater. Technol.* (2018) **3**:1700274.
- 337 25. Zeng Q-Y, Xi M, Xu W, Li X-J. Preparation of titanium dioxide nanotube arrays on titanium  
338 mesh by anodization in (NH<sub>4</sub>)<sub>2</sub>SO<sub>4</sub>/NH<sub>4</sub>F electrolyte. *Mater. Corros.* (2013) **64**:1001–1006.
- 339 26. Gulati K, Santos A, Findlay D, Losic D. Optimizing Anodization Conditions for the Growth of  
340 Titania Nanotubes on Curved Surfaces. *J. Phys. Chem. C* (2015) **119**:16033–16045.
- 341 27. He W, Qiu J, Zhuge F, Li X, Lee J-H, Kim Y-D, Kim H-K, Hwang Y-H. Advantages of using Ti-  
342 mesh type electrodes for flexible dye-sensitized solar cells. *Nanotechnology* (2012) **23**:225602.
- 343 28. Chun KY, Park BW, Sung YM, Kwak DJ, Hyun YT, Park MW. Fabrication of dye-sensitized  
344 solar cells using TiO<sub>2</sub>-nanotube arrays on Ti-grid substrates. *Thin Solid Films* (2009) **517**:4196–  
345 4198.
- 346 29. Gerosa M, Sacco A, Scalia A, Bella F, Chiodoni A, Quaglio M, Tresso E, Bianco S. Toward  
347 Totally Flexible Dye-Sensitized Solar Cells Based on Titanium Grids and Polymeric Electrolyte.  
348 *IEEE J. Photovolt.* (2016) **6**:498–505.

**Enhanced Electrochemical Performances of Self-Organized TiO<sub>2</sub> Nanotubes  
Fabricated by Anodization of Ti Grid**

- 349 30. Liu Z, Subramania V (Ravi), Misra M. Vertically Oriented TiO<sub>2</sub> Nanotube Arrays Grown on Ti  
350 Meshes for Flexible Dye-Sensitized Solar Cells. *J. Phys. Chem. C* (2009) **113**:14028–14033.
- 351 31. Motola M, Dworniczek E, Satrapinskyy L, Chodaczek G, Grzesiak J, Gregor M, Plecenik T,  
352 Nowicka J, Plesch G. UV light-induced photocatalytic, antimicrobial, and antibiofilm  
353 performance of anodic TiO<sub>2</sub> nanotube layers prepared on titanium mesh and Ti sputtered on  
354 silicon. *Chem. Pap* (2019) **73**:1163–1172.
- 355 32. Martin M, Leonid S, Tomáš R, Jan Š, Jaroslav K, Mariana K, Michaela J, František P, Gustav P.  
356 Anatase TiO<sub>2</sub> nanotube arrays and titania films on titanium mesh for photocatalytic NOX removal  
357 and water cleaning. *Catal.Today* (2017) **287**:59–64.
- 358 33. Rustomji CS, Frandsen CJ, Jin S, Tauber MJ. Dye-Sensitized Solar Cell Constructed with  
359 Titanium Mesh and 3-D Array of TiO<sub>2</sub> Nanotubes. *J. Phys. Chem. B* (2010) **114**:14537–14543.
- 360 34. Liao J, Lin S, Zhang L, Pan N, Cao X, Li J. Photocatalytic Degradation of Methyl Orange Using  
361 a TiO<sub>2</sub>/Ti Mesh Electrode with 3D Nanotube Arrays. *ACS Appl. Mater. Interfaces* (2012) **4**:171–  
362 177.
- 363 35. Ozkan S, Nguyen NT, Mazare A, Cerri I, Schmuki P. Controlled spacing of self-organized anodic  
364 TiO<sub>2</sub> nanotubes. *Electrochem. Commun.* (2016) **69**:76–79.
- 365 36. Plylahan N, Letiche M, Barr MKS, Djenizian T. All-solid-state lithium-ion batteries based on  
366 self-supported titania nanotubes. *Electrochem. Commun.* (2014) **43**:121–124.
- 367 37. Macak JM, Tsuchiya H, Taveira L, Aldabergerova S, Schmuki P. Smooth anodic TiO<sub>2</sub> nanotubes.  
368 *Angew. Chem. Int. Ed.*(2005) **44**:7463–7465.
- 369 38. Macak JM, Schmuki P. Anodic growth of self-organized anodic TiO<sub>2</sub> nanotubes in viscous  
370 electrolytes. *Electrochim. Acta* (2006) **52**:1258–1264.
- 371 39. Song Y-Y, Lynch R, Kim D, Roy P, Schmuki P. TiO<sub>2</sub> Nanotubes: Efficient Suppression of Top  
372 Etching during Anodic Growth Key to Improved High Aspect Ratio Geometries. *Electrochem*  
373 *Solid-State Lett.* (2009) **12**:C17–C20.
- 374 40. Kirchgeorg R, Kallert M, Liu N, Hahn R, Killian MS, Schmuki P. Key factors for an improved  
375 lithium ion storage capacity of anodic TiO<sub>2</sub> nanotubes. *Electrochim. Acta* (2016) **198**:56–65.
- 376 41. Mor GK, Varghese OK, Paulose M, Shankar K, Grimes CA. A review on highly ordered,  
377 vertically oriented TiO<sub>2</sub> nanotube arrays: Fabrication, material properties, and solar energy  
378 applications. *Sol. Energ. Mat. Sol.C.* (2006) **90**:2011–2075.
- 379 42. Altomare M, Pozzi M, Allieta M, Bettini LG, Selli E. H<sub>2</sub> and O<sub>2</sub> photocatalytic production on  
380 TiO<sub>2</sub> nanotube arrays: Effect of the anodization time on structural features and photoactivity.  
381 *Appl.Catal. B: Environmental* (2013) **136–137**:81–88.
- 382 43. Liu Z, Zhang Q, Zhao T, Zhai J, Jiang L. 3-D vertical arrays of TiO<sub>2</sub> nanotubes on Ti meshes:  
383 Efficient photoanodes for water photoelectrolysis. *J. Mater. Chem* (2011) **21**:10354–10358.

## Enhanced Electrochemical Performance of Electropolymerized Self-Organized TiO<sub>2</sub> Nanotubes Fabricated by Anodization of Ti Grid

- 384 44. Zhang Z-J, Zeng Q-Y, Chou S-L, Li X-J, Li H-J, Ozawa K, Liu H-K, Wang J-Z. Tuning three-  
385 dimensional TiO<sub>2</sub> nanotube electrode to achieve high utilization of Ti substrate for lithium  
386 storage. *Electrochim. Acta* (2014) **133**:570–577.
- 387 45. Ferrari IV, Braglia M, Djenizian T, Knauth P, Di Vona ML. Electrochemically engineered single  
388 Li-ion conducting solid polymer electrolyte on titania nanotubes for microbatteries. *J.Power*  
389 *Sources* (2017) **353**:95–103.
- 390 46. Salian GD, Lebouin C, Demoulin A, Lepihin MS, Maria S, Galeyeva AK, Kurbatov AP,  
391 Djenizian T. Electrodeposition of polymer electrolyte in nanostructured electrodes for enhanced  
392 electrochemical performance of thin-film Li-ion microbatteries. *J.Power Sources* (2017)  
393 **340**:242–246.
- 394 47. Plylahan N, Maria S, Phan TN, Letiche M, Martinez H, Courrèges C, Knauth P, Djenizian T.  
395 Enhanced electrochemical performance of Lithium-ion batteries by conformal coating of polymer  
396 electrolyte. *Nanoscale Res. Lett.*(2014) **9**:544.
- 397 48. Sugiawati VA, Vacandio F, Ein-Eli Y, Djenizian T. Electrodeposition of polymer electrolyte into  
398 carbon nanotube tissues for high performance flexible Li-ion microbatteries. *APL Mater.*(2019)  
399 **7**:031506.
- 400 49. Braglia M, Ferrari IV, Djenizian T, Kaciulis S, Soltani P, Di Vona ML, Knauth P. Bottom-Up  
401 Electrochemical Deposition of Poly(styrene sulfonate) on Nanoarchitected Electrodes. *ACS*  
402 *Appl. Mater. Interfaces* (2017) **9**:22902–22910.
- 403 50. Plylahan N, Letiche M, Samy Barr MK, Ellis B, Maria S, Phan TNT, Bloch E, Knauth P,  
404 Djenizian T. High energy and power density TiO<sub>2</sub> nanotube electrodes for single and complete  
405 lithium-ion batteries. *J.Power Sources* (2015) **273**:1182–1188.
- 406 51. Ortiz GF, Hanzu I, Djenizian T, Lavela P, Tirado JL, Knauth P. Alternative Li-Ion Battery  
407 Electrode Based on Self-Organized Titania Nanotubes. *Chem Mater* (2009) **21**:63–67.

408

409

Figure 1.TIF

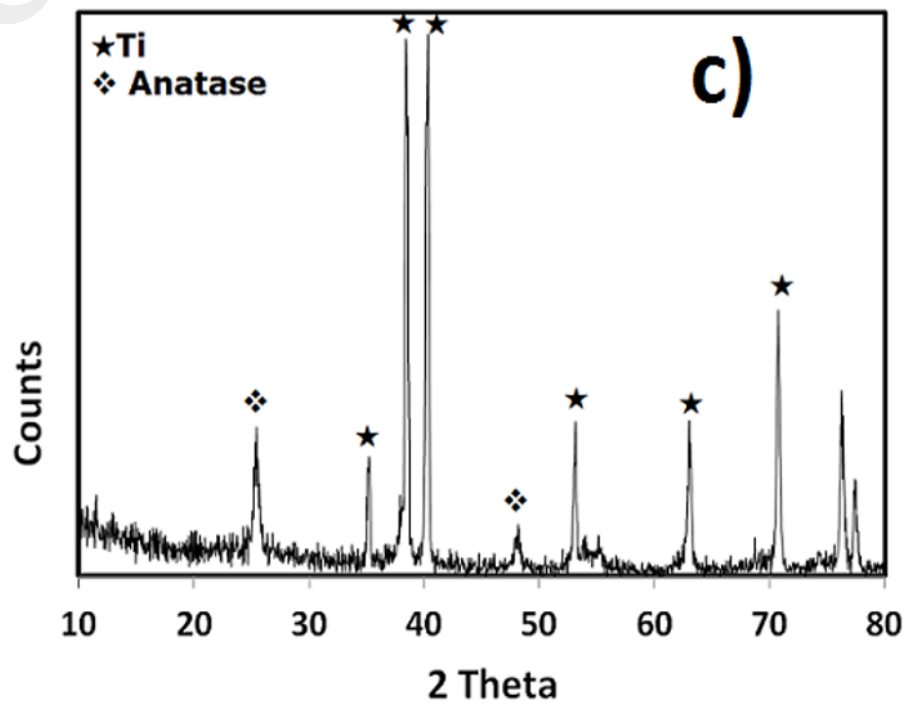
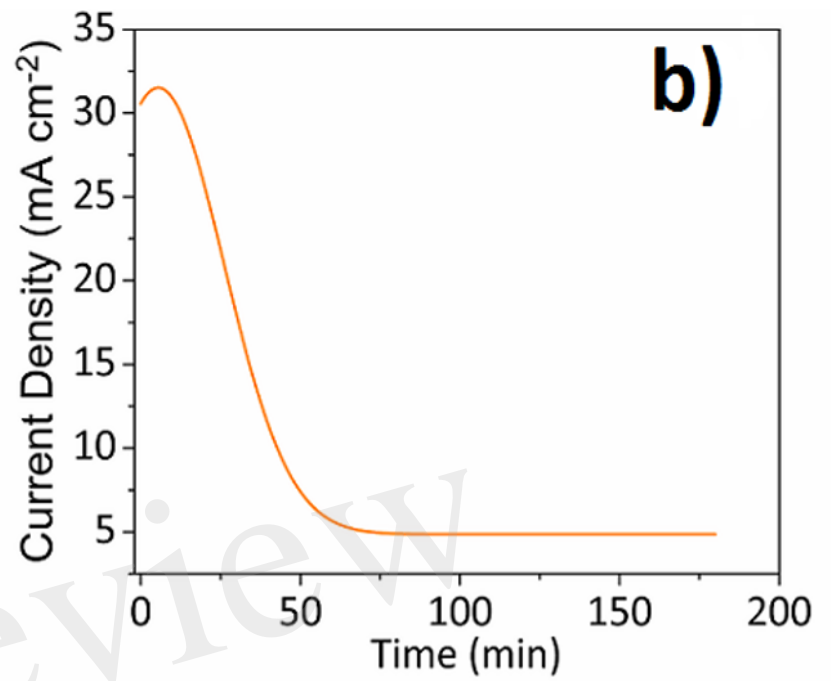
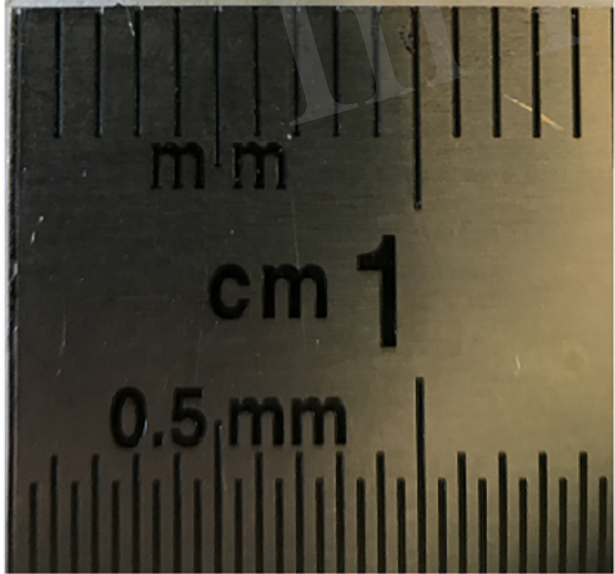
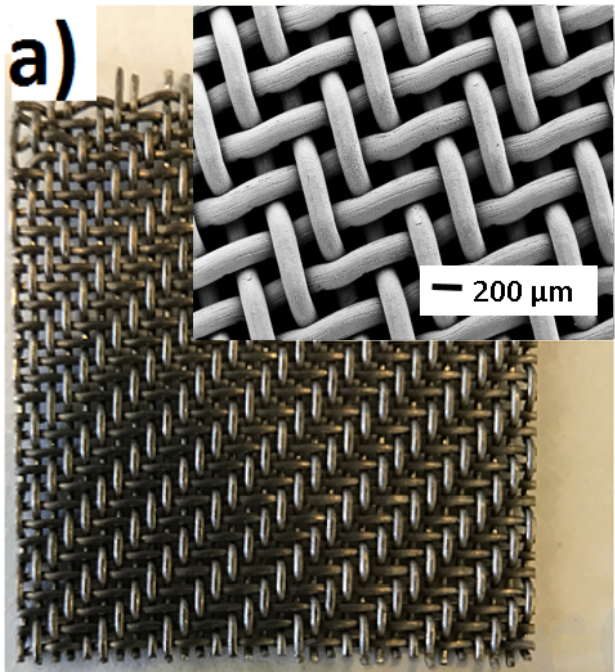


Figure 2.TIF

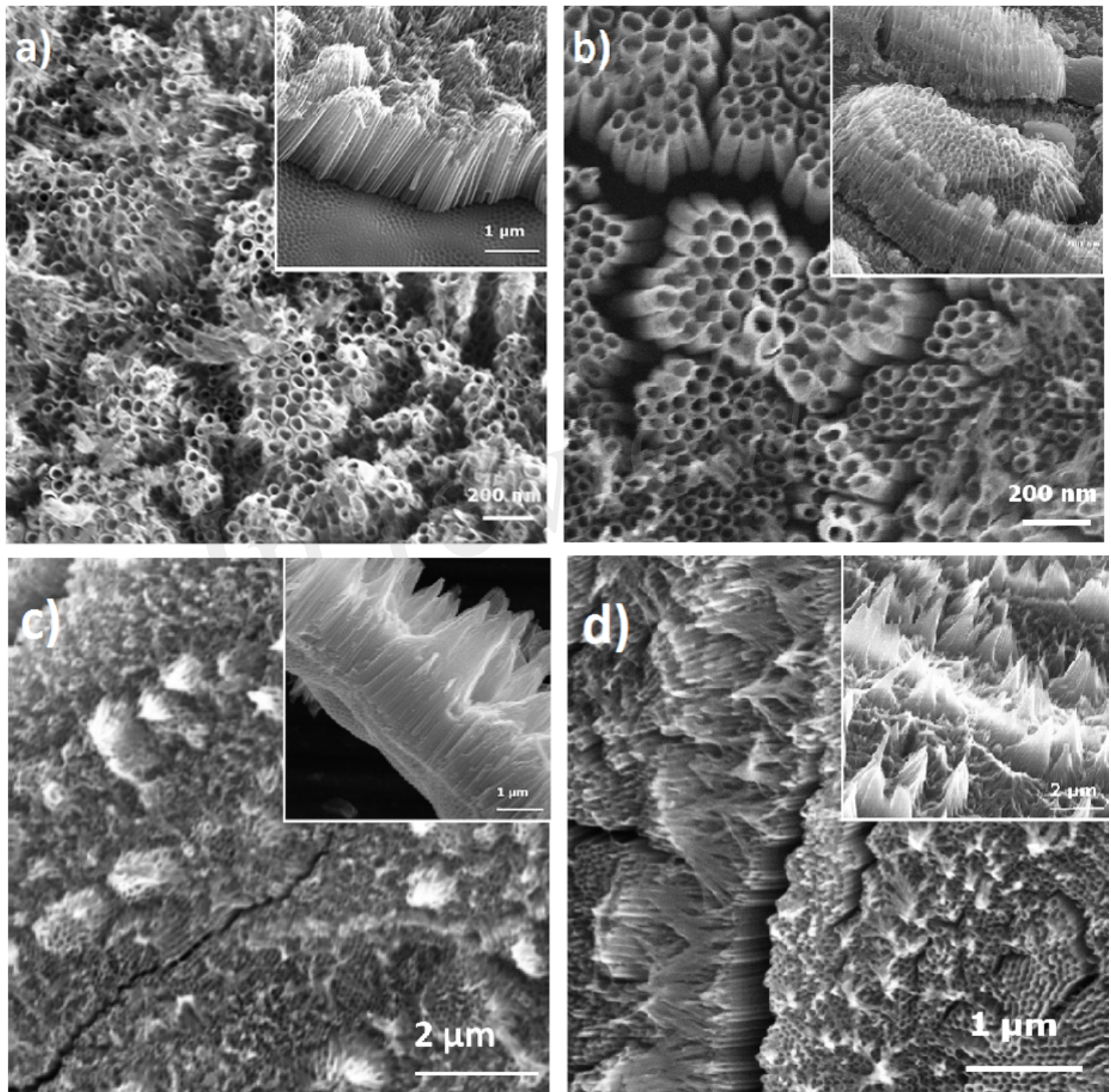


Figure 3.TIF

In review

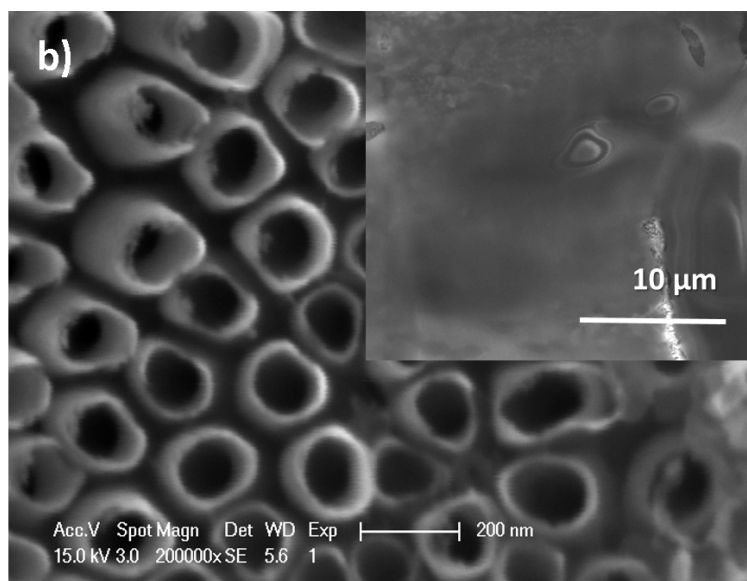
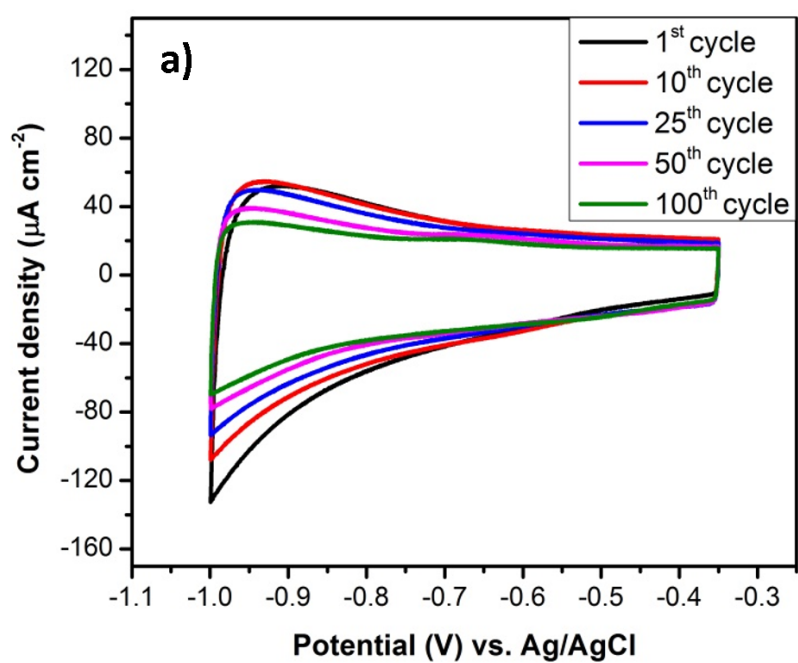




Figure 4.TIF

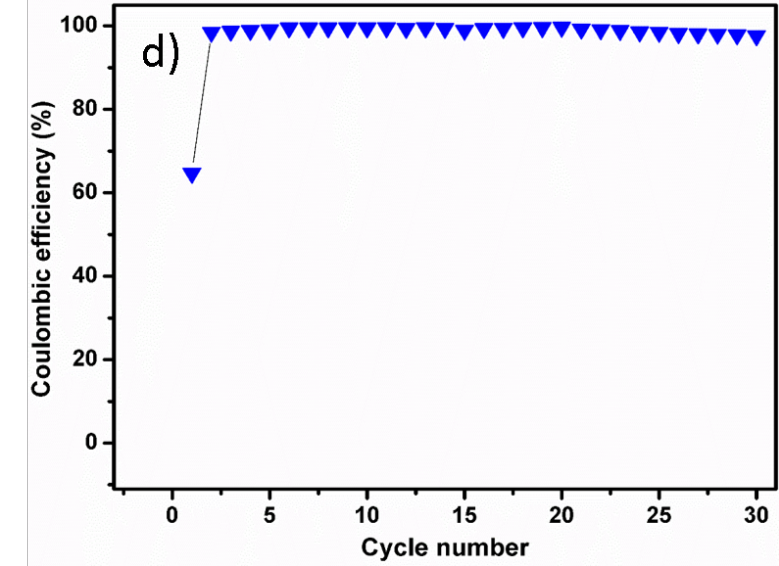
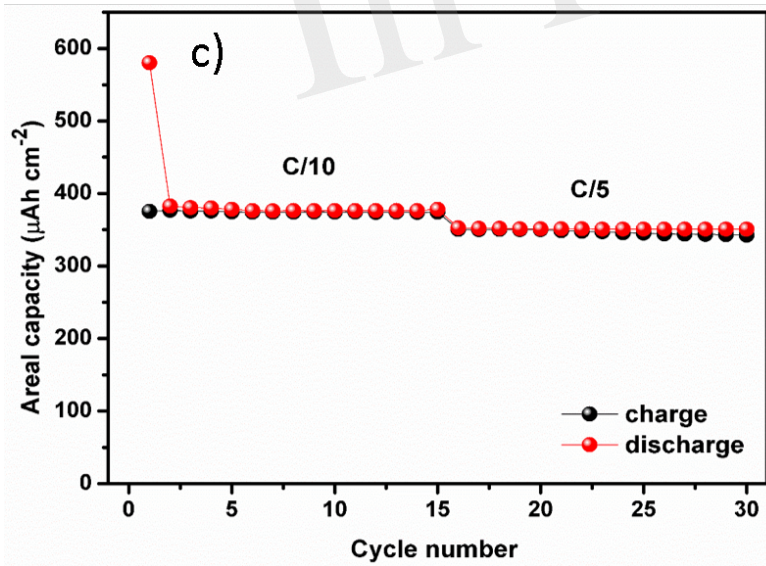
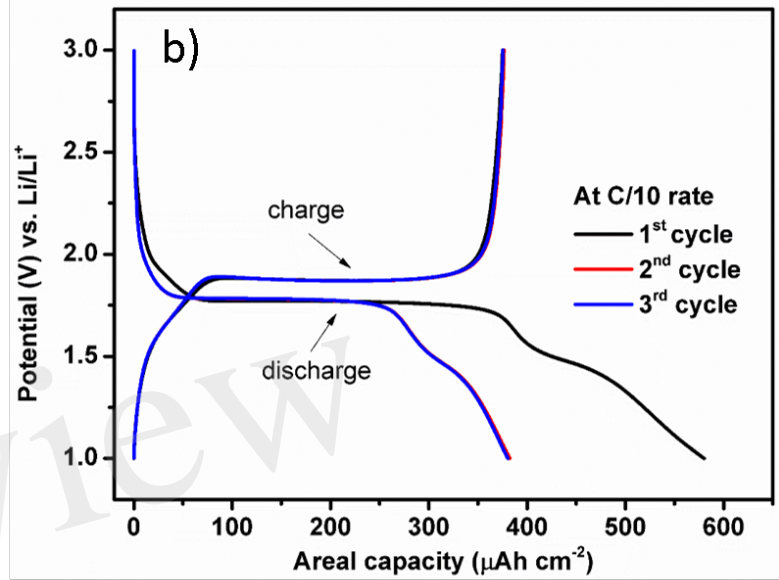
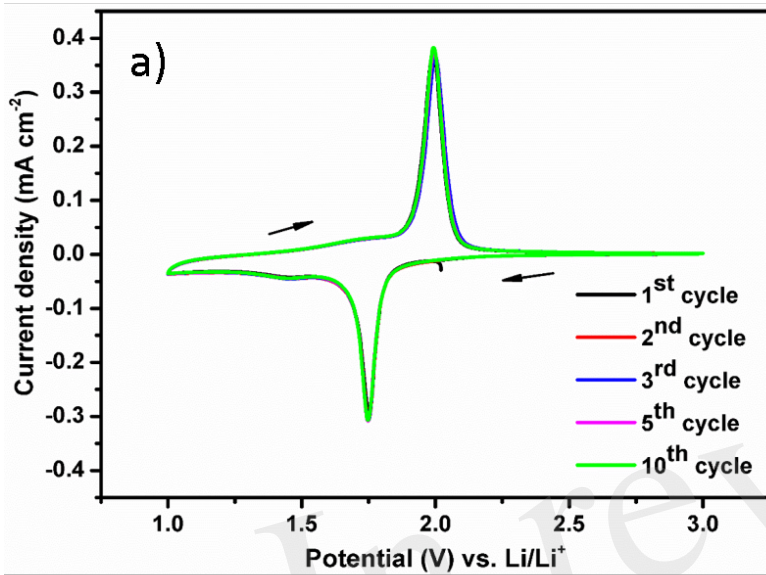


Figure 6.TIF

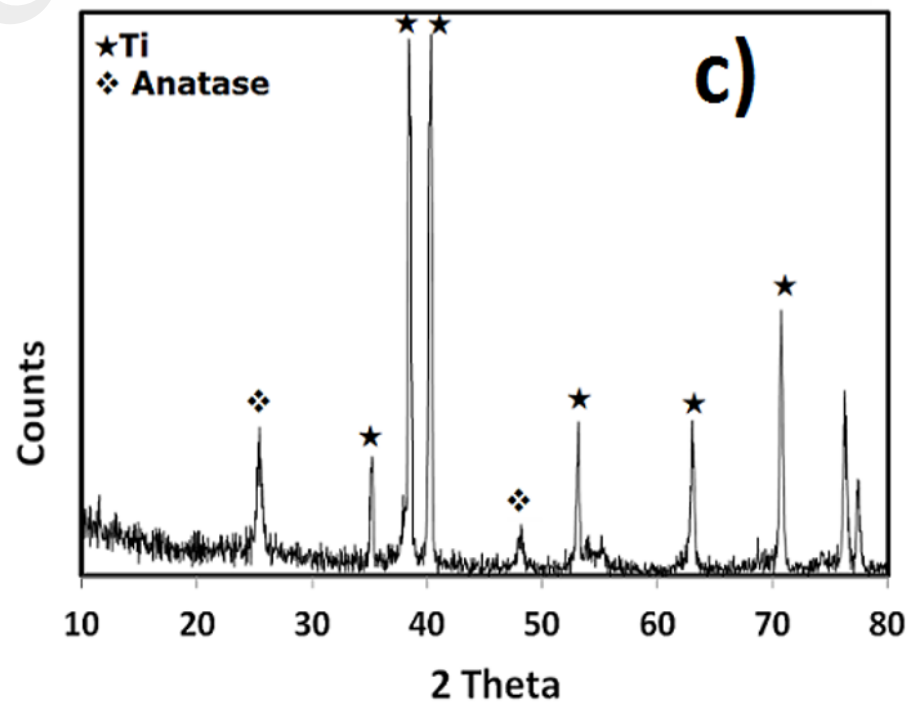
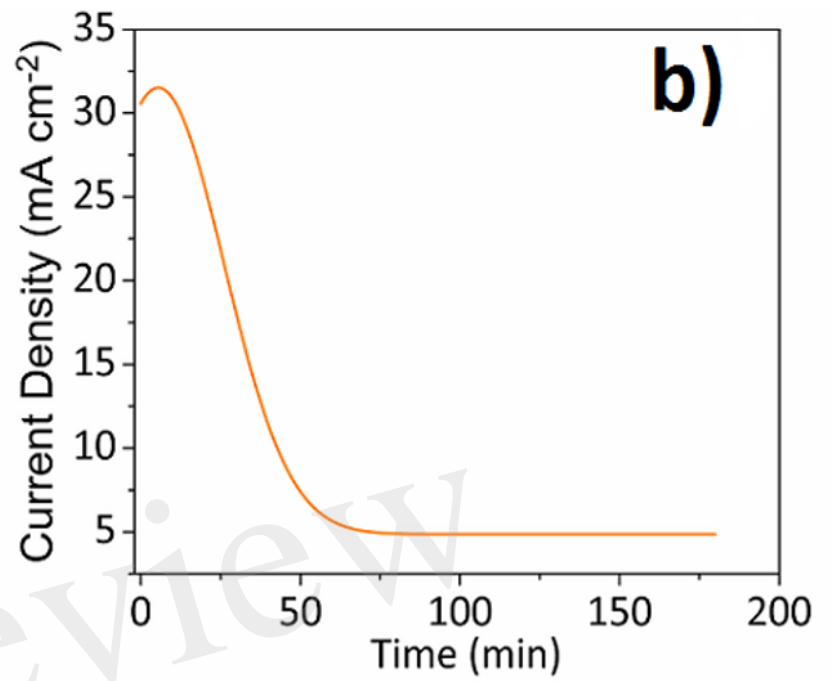
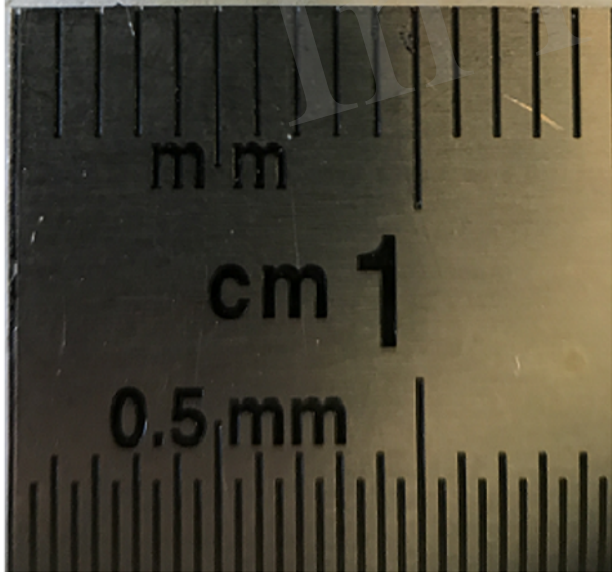
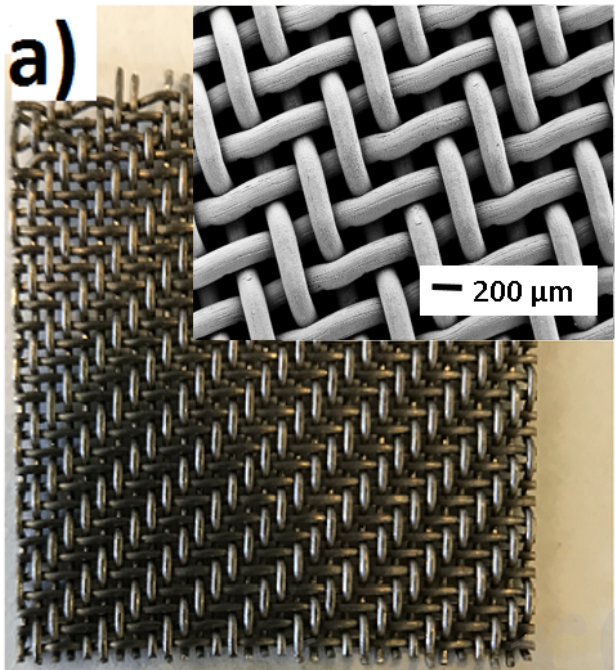


Figure 7.TIF

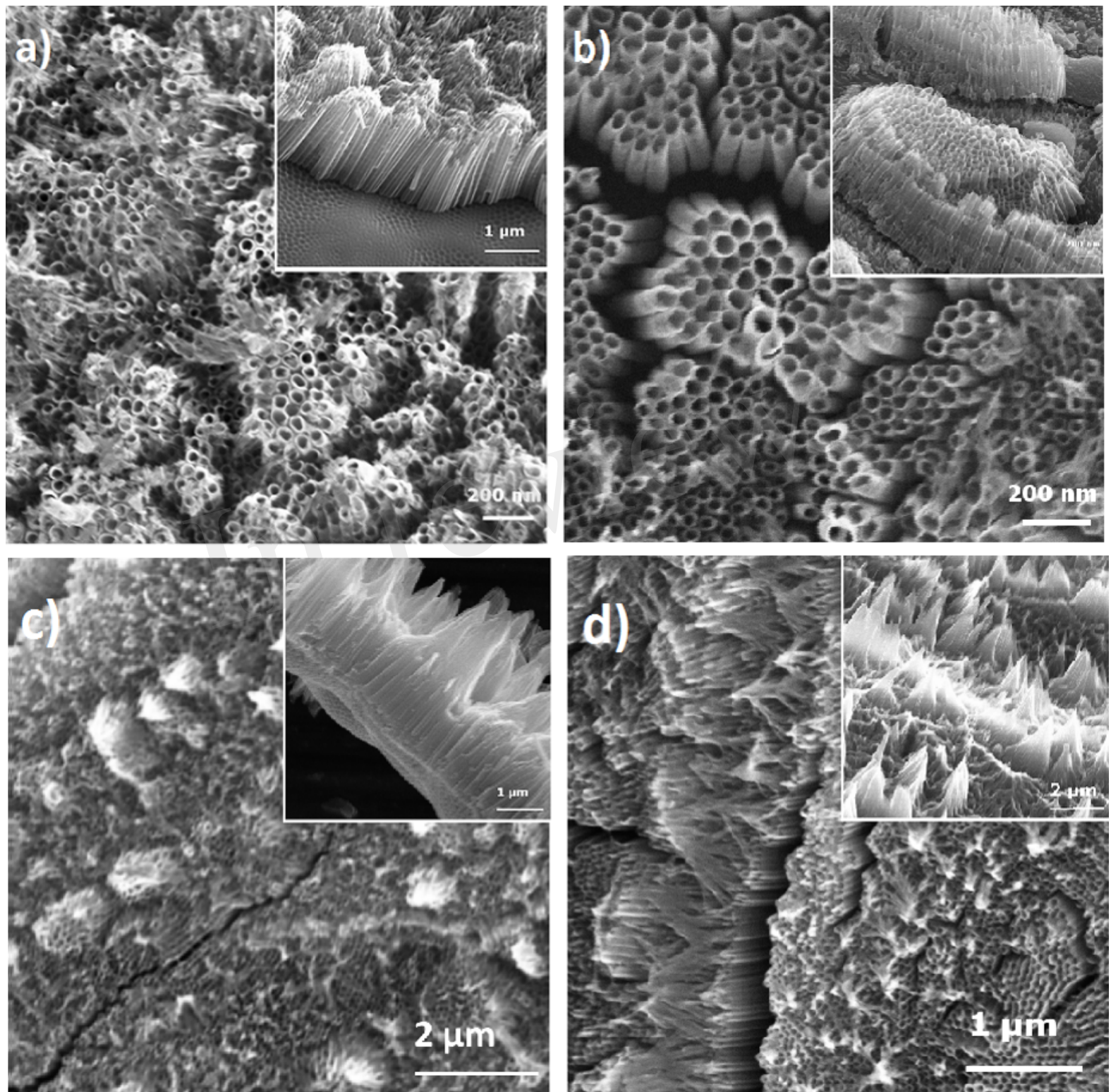


Figure 8.TIF

In review

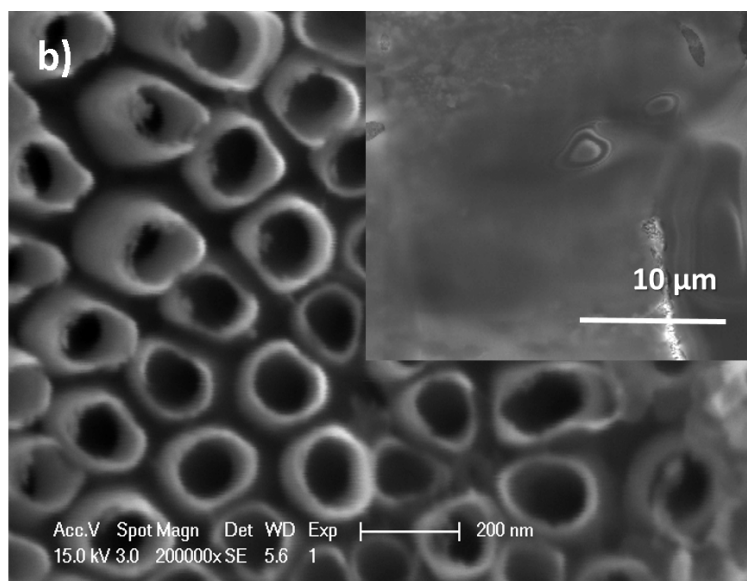
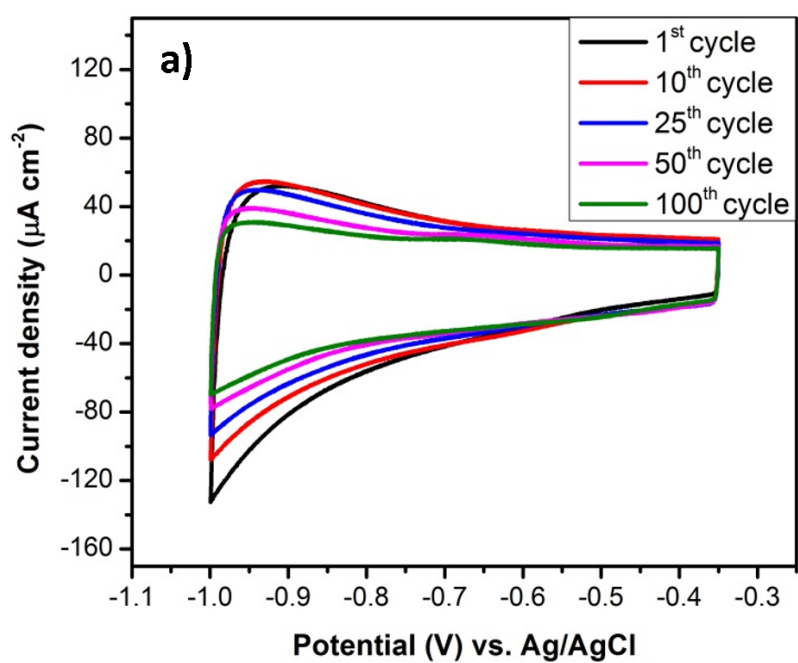


Figure 9.TIF

